Water Science & Technology

Water Science & Technology Vol 86 No 1, 194 doi: 10.2166/wst.2022.193

Investigation on the feasibility of recycled polyvinylidene difluoride polymer from used membranes for removal of methylene blue: experimental and DFT studies

Raj Vardhan Patel [a], Gopika B. Raj [a,b], Shweta Chaubey [a] and Anshul Yadav [a,*]

[a] CSIR-Central Salt and Marine Chemicals Research Institute, Bhavnagar 364002, India
[b] Centre for Bio-Polymer Science and Technology (unit of CIPET), Kochi 683501, India
*Corresponding author. E-mail: anshuly@csmcri.res.in

RVP, 0000-0003-1309-1573; SC, 0000-0003-4390-0300; AY, 0000-0003-1380-2662

ABSTRACT

This study reports the feasibility of recycled polyvinylidene difluoride (PVDF) beads to decolourize methylene blue (MB) from aqueous streams. The beads were characterized using scanning electron microscopy (SEM), X-ray powder diffraction (XRD), thermogravimetric analysis (TGA), and Fourier transform infrared spectroscopy (FT-IR) for its morphological and structural analysis. The effect of various process parameters such as adsorbent dose, initial concentration, contact time, and pH was studied. The first principle density functional theory (DFT) calculations were performed to investigate the underlying mechanism behind the adsorption process. The MB dye adsorption on recycled PVDF beads followed the pseudo-second-order kinetics and Langmuir isotherm, indicating the adsorption was chemical and monolayer. The maximum adsorption capacity obtained was 27.86 mg g^{-1}. The adsorption energy of MB-PVDF predicted from the DFT study was –64.7 kJ mol^{-1}. The HOMO-LUMO energy gap of PVDF decreased from 9.42 eV to 0.50 eV upon interaction with MB dye due to the mixing of molecular orbitals. The DFT simulations showed that the interaction of the MB dye molecule was from the electronegative N atom of the MB dye molecule, implying that electrostatic interactions occurred between the recycled PVDF beads and the positively charged quaternary ammonium groups in MB dye. The present study demonstrates the potential of recycled PVDF beads for a low-cost dye removal technique from textile wastewater.

Key words: adsorption, density functional theory, methylene blue, polyvinylidene difluoride, textile wastewater

HIGHLIGHTS

- Experiments and DFT calculations were performed to evaluate the binding of MB dye to PVDF beads synthesized from used membranes.
- The adsorption of MB dye on PVDF beads was monolayer and chemical in nature, with a maximum adsorption capacity of 27.86 mg g^{-1}.
- The DFT study predicted the adsorption energy of 64.7 kJ mol^{-1} for MB-PVDF, indicating the strong interaction between MB dye and PVDF.
- The study demonstrated the potential of recycled PVDF beads for a low-cost dye removal technique.

GRAPHICAL ABSTRACT

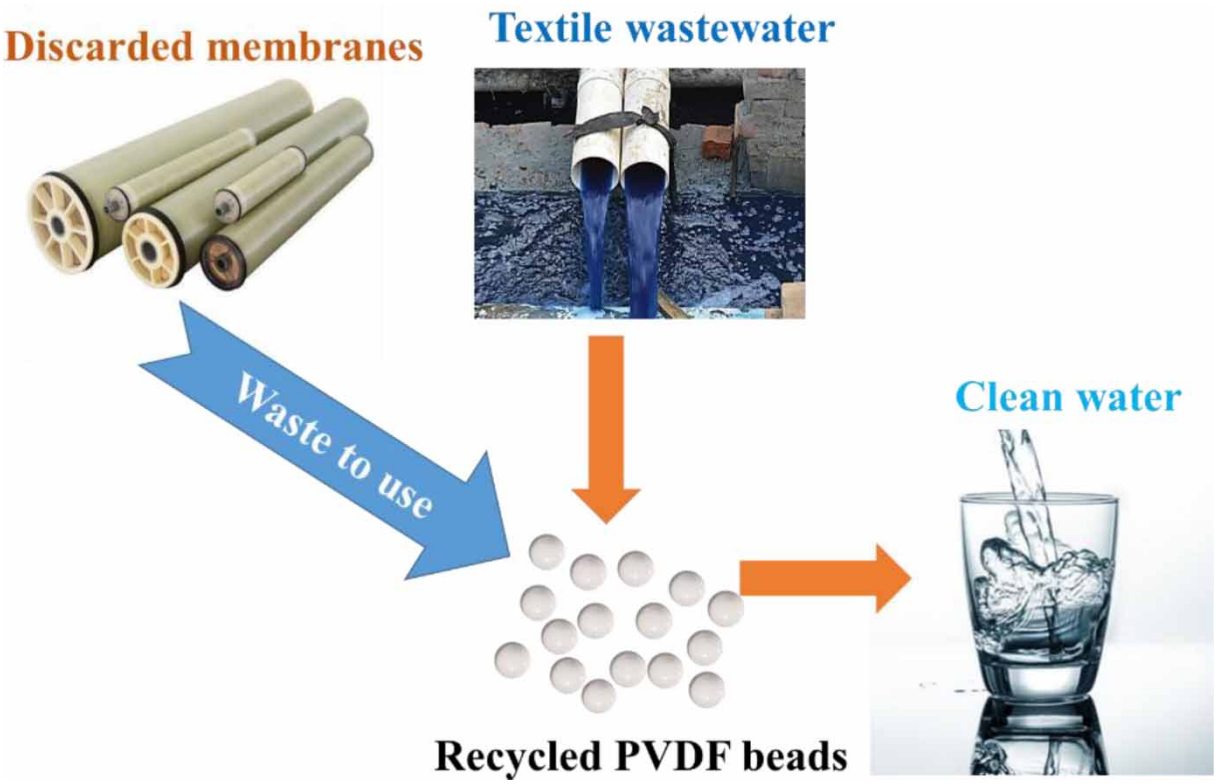

1. INTRODUCTION

In the past few decades, membranes have been used excessively for water and wastewater treatment, leading to the increased disposal of waste membranes (Ezugbe *et al.* 2020). At the current rate, the disposal of membrane modules exhibits significant and escalating detrimental impacts, leading to the need to limit the direct disposal of these modules. Currently, used membranes are disposed of in landfills or incinerated. However, these methods are not completely dependable because of the environmental impacts. The discarded membranes can be recycled and reused for different separation processes with less demanding specifications with some post-processing. Several methods have been employed to recycle membranes, such as chemical cleaning (Yi *et al.* 2017), physical cleaning and backwashing (Park *et al.* 2018), and direct recycling of the various module components (Lawler *et al.* 2012). Paula *et al.* (2017) examined the technological viability of desalination membrane recycling by chemical oxidation. The end-of-life membranes deteriorate due to fouling, biofouling, etc. The polymer recovered from the membranes can be used as adsorbents to remove hazardous contaminants from wastewater. However, very few studies are available where polymers recovered from waste membranes have been used for adsorption (Zwain *et al.* 2014).

Synthetic dyes are found in huge quantities in textile and dye processing industrial effluent, posing a significant environmental threat. Many industries produce these dyes, including textiles, printing, paper, and plastic (Ngulube *et al.* 2017; Yadav *et al.* 2021a, 2021b, 2021c). Methylene blue (MB) is a cationic dye found in considerable quantities in textile effluent released into the environment without the significant treatment of its release into the surrounding ecosystem (Yadav *et al.* 2021a, 2021b, 2021c). At present, biological, physical, and chemical methods are employed for textile dye removal from wastewater (Yaseen & Scholz 2019). However, there are many shortcomings associated with these traditional technologies for dye removal, including chemical release, secondary sludge, high initial cost, and low decolourization efficiency (Piaskowski *et al.* 2018). Adsorption is one of the most economical, effective, and simple processes for the decolourization of textile water. Furthermore, it shows a wide range of materials such as nanomaterials, carbonaceous materials, bioadsorbents, etc. (Tran *et al.* 2019).

In recent years, polymeric adsorbents have become popular as an alternative to traditional adsorbents such as clays and activated carbon due to their tunable physicochemical characteristics, structural variability, reusability, and selectivity (Mok *et al.* 2020; Yadav & Sinha 2021). Zheng *et al.* (2018) studied the feasibility of polymer-functionalized magnetic nanoparticles for MB removal. Fe_3O_4-incorporated carboxyl functionalized nanoporous polymer showed high performance for MB dye adsorption from wastewater (Su *et al.* 2018). Carbon nanotubes-based polymer nanocomposites were found to be suitable for the adsorption of MB from the aqueous solution (Gan *et al.* 2020). Several researchers have used waste material to remove dyes from textile wastewater. For instance, Kiran *et al.* (2020) used agro-industrial waste (palm date stones) to adsorb basic violet 3 and basic red 2 from textile wastewater with high removal efficiency (77%- basic red 2, 93% basic violet 3). Wong *et al.* (2020) used coffee waste modified with polyethyleneimine to adsorb dye from textile wastewater with an adsorption capacity of 34.36 mg g^{-1} (Congo red) and 77.52 mg g^{-1} (reactive black 5). Temesgen *et al.* (2018) used activated orange and banana peel to eliminate reactive red dye from textile industry wastewater with very high removal efficiency (>89%). Vecino *et al.* (2015) synthesized biocomposites from vineyard waste entrapped in calcium alginate hydrogel beads to eliminate dye from wastewater and achieved 74.6% dye removal efficiency. Polyvinyledienefluoride (PVDF) and its co-polymer have been widely used to treat textile wastewater. Zhang *et al.* (2019) fabricated a PVDF/GO/ZnO composite to remove MB dye through photocatalytic degradation, achieving a removal efficiency of 86.84%.

A careful literature survey shows that PVDF effectively adsorbs MB dye from an aqueous stream. Hence, in this study, PVDF polymer from a recycled membrane was used as an adsorbent for removing MB dye from textile wastewater. The PVDF beads obtained from recycled membranes were characterized using scanning electron microscopy (SEM), X-ray powder diffraction (XRD), thermogravimetric analysis (TGA), and Fourier transform infrared spectroscopy (FT-IR) for morphological and structural analysis. A parametric study was performed to study the effect of varying adsorbent dose, initial concentration, contact time, and pH on the beads' adsorption capacity and removal efficiency. Moreover, density functional theory (DFT) calculations, adsorption isotherm, and kinetics were studied to identify the adsorption process' mechanism.

2. MATERIALS AND METHODS

2.1. Materials

The recycled PVDF was obtained from used membranes. Dimethylformamide (DMF) solvent (purity ~99.5%) was purchased from Spectrochem Pvt. Ltd Mumbai, India. MB dye (purity ~82%) was procured from NICE chemicals Pvt. Ltd, India. Deionized (DI) water (~18 M Ω) was obtained from the Millipore Q BIOCEL unit, Millipore.

2.2. Adsorbent synthesis

The recycled membrane was washed thoroughly, and the PVDF (16 g) was delaminated from the fabric and dissolved in DMF solvent (100 ml) for 6 h at 60 °C under constant stirring. The PVDF solution (16 wt.%) was taken in a clean syringe and added dropwise to a beaker filled with DI water (coagulation bath). The recycled PVDF polymer precipitated in the form of spherical beads. The beads were kept in the coagulation bath overnight to complete the phase inversion process.

2.3. Adsorption experiments

Adsorption experiments were performed to investigate recycled PVDF beads' adsorption capacity and removal efficiency for MB dye. The batch experiments were performed by varying different parameters, such as adsorbent dosage, pH, initial dye concentration, and contact time to assess the optimal conditions for the adsorption process. To examine the effect of the adsorbent dose for MB dye, adsorption was varied from 0.2 to 3 g L^{-1}. To assess the effect of MB dye concentration on the recycled PVDF beads, the solution concentration was varied from 10 to 250 ppm. The MB dye solution's pH was varied from 2 to 12 to assess its effect. The pH adjustment of the dye solution was achieved using 0.1 N HCl or 0.1 N NaOH. To optimize the adsorption time, the contact time of the adsorbent was varied in the range of 5–240 mins. The adsorption capacity and removal efficiency was estimated from the equations shown below:

$$\text{Adsorption capacity } (q_e) = \left(\frac{C_i - C_e}{m}\right) \times V \tag{1}$$

$$\textit{Removal efficiency} = \frac{(C_i - C_e)}{C_i} \times 100 \tag{2}$$

where q_e – equilibrium adsorption capacity, C_i – MB dye's initial concentration, C_e – MB dye's equilibrium concentration, m – mass of the recycled PVDF beads, and V – volume of MB dye's solution.

2.4. Adsorption kinetics

Time is critical in studying an adsorbent's adsorption kinetics as the adsorption process changes with time. The kinetics of the adsorption process help predict the pathway by which the adsorption process must have taken place (Ivanets *et al.* 2019). In the case of the adsorption, the physiochemical characteristics of the adsorbent and system parameters such as temperature and contact time determine the nature of the process (Dindorkar *et al.* 2022a). The amount of dye adsorbed at time t, denoted by q_t, was calculated by using the following equation:

$$q_t = \frac{(C_i - C_t)}{m} \times V \tag{3}$$

where q_t – adsorbed ions amount per unit mass of the adsorbent in time t, m – mass of adsorbent used, and C_t – dye's concentration at instant t. To investigate the adsorption kinetics in this study, the non-linear pseudo-first-order (PFO) and the pseudo-second-order (PSO) kinetic models were used. The non-linear form of the PFO and PSO equation is given below:

$$\frac{dq_t}{dt} = k_1(q_e - q_t) \tag{4}$$

$$\frac{dq_t}{dt} = k_2(q_e - q_t)^2 \tag{5}$$

The integration of Equations (4) and (5) for the boundary conditions ($t = 0$, $q_t = 0$ and $t = t$, $q_e = q_t$) results in the following equations

$$q_t = \ q_e(1 - e^{-k_1 t}) \tag{6}$$

$$q_t = \frac{k_2 q_e^2 t}{1 + k_2 q_e t} \tag{7}$$

where q_t – amount of adsorbed ions per unit adsorbent at instant t, k_1 – PFO constant, and k_2 – rate constant of the PSO.

2.5. Adsorption isotherm

The adsorption isotherms provide the equilibrium concentration between the adsorbed and unadsorbed phase at a particular condition. The Langmuir and Freundlich isotherms were chosen for this investigation. The Langmuir adsorption (monolayer adsorption) isotherm assumes that the adsorption occurs within the adsorbent at specific homogeneous sites, while the Freundlich isotherms assume the heterogeneous adsorption sites (multilayer adsorption) (Patel and Yadav, 2022). The non-linear form of the Langmuir isotherm is described below.

$$q_e = \frac{q_m C_e b}{1 + bC_e} \tag{8}$$

where b – constant for Langmuir isotherm, q_m – maximum adsorption capacity, C_e – equilibrium dye concentration. The non-linear form of the equation of Freundlich isotherm is described as:

$$q_e = \ K_F C_e^{\frac{1}{n}} \tag{9}$$

where n – intensity and K_F – Freundlich coefficient.

2.6. Computational details

The Gaussian 09 package was used to perform the first-principle DFT calculations (Wallingford CT 2013). For the geometry optimizations, a hybrid CAM-B3LYP functional was used with an IEF-PCM model to reflect the long-range corrections (Yanai *et al.* 2004; Caldeweyher *et al.* 2017). Theoretical FT-IR spectra, HOMO-LUMO distribution and density of states (DOS) plots were obtained using GaussSum (O'Boyle *et al.* 2008) software. The basis set superposition error (BSSE) was incorporated while calculating adsorption energy using counterpoise correction (Boys & Bernardi 1970). The following equation was used to calculate the adsorption energy.

$$E_{MB-PVDF} = E_{MB+PVDF} - (E_{MB} + E_{PVDF}) \tag{10}$$

where the term, $E_{MB-PVDF}-$ total energy of the MB-PVDF complex cluster, E_{PVDF} – energy of PVDF and $E_{MB}-$ energy of the MB dye. The reactivity descriptors (chemical hardness, chemical potential, and electrophilicity index) were evaluated using Koopmans' theorem (Yadav & Dindorkar 2022a, 2022b).

2.7. Characterization techniques

The morphological characteristics of the adsorbent composite beads were studied from SEM (JEOL JSM 7100F). The adsorbent IR spectrography was performed using the Perkin Elmer FTIR spectrometer (USA). The thermogravimetric analysis (TGA) was accomplished with a thermogravimetric analyzer (Mettler Toledo) with nitrogen flow at a heating rate of 10° C min^{-1}. The measurement of MB dye concentrations was assessed using a UV-Vis spectrophotometer by constructing a calibration curve, and for pH monitoring, a Eutech PC2700 multiparameter device (Shimadzu, Japan) was used. The characteristic absorbance of MB dye at 663 nm was chosen to study the decolourization during the adsorption.

3. RESULTS AND DISCUSSIONS

3.1. Characterization studies

Figure 1 illustrates the surface and cross-sectional morphology of recycled PVDF beads. The surface morphology of the beads was rough and porous. The recycled PVDF beads' internal porous and spongy cross-section morphology was attributed to the solvent and non-solvent exchange during the phase inversion process (Zahirifar *et al.* 2019). The recycled PVDF beads' rough and porous morphology will provide a larger surface area and an adsorption process with more active sites.

TGA was conducted to study the thermal stability of the synthesized recycled PVDF beads (Figure 2(a)). Till 427 °C, there was a loss of ~3% mass, attributed to the evaporation of humidity entrapped in the beads. When the temperature reached 427 °C, the residual mass declined rapidly to 34%, attributed to the thermal degradation of the PVDF polymer's –(C2H2F2)n– units. Hence, it was concluded that the synthesized beads were stable up to 427 °C, favouring non-isothermal adsorption.

Figure 2(b) shows the XRD spectra of the recycled PVDF beads. The sharp peaks in XRD spectra at $2\theta = 17.75°$ and 22.80° corresponded to (100) and (110) α-crystal diffractions recycled PVDF, respectively (Janakiraman *et al.* 2016). The sharp peaks

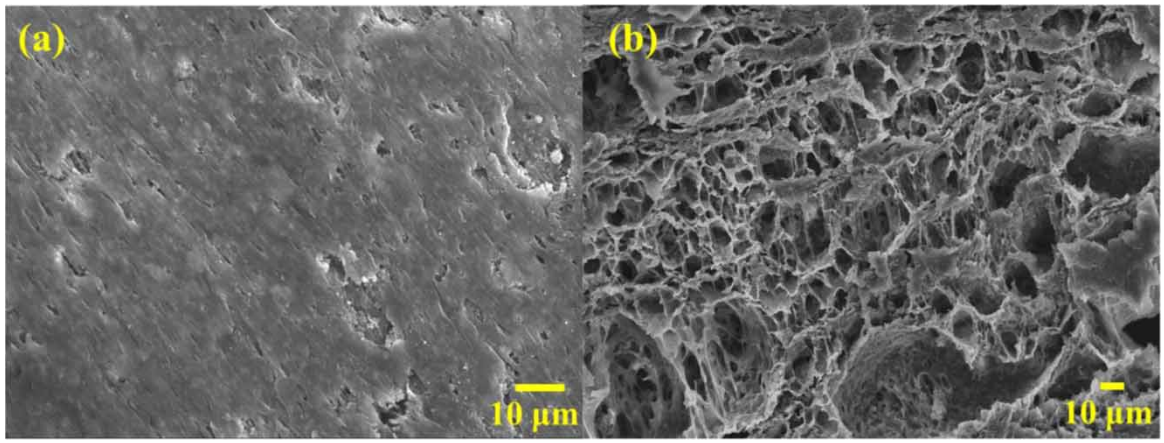

Figure 1 | SEM images of recycled PVDF beads (a) surface and (b) cross-section.

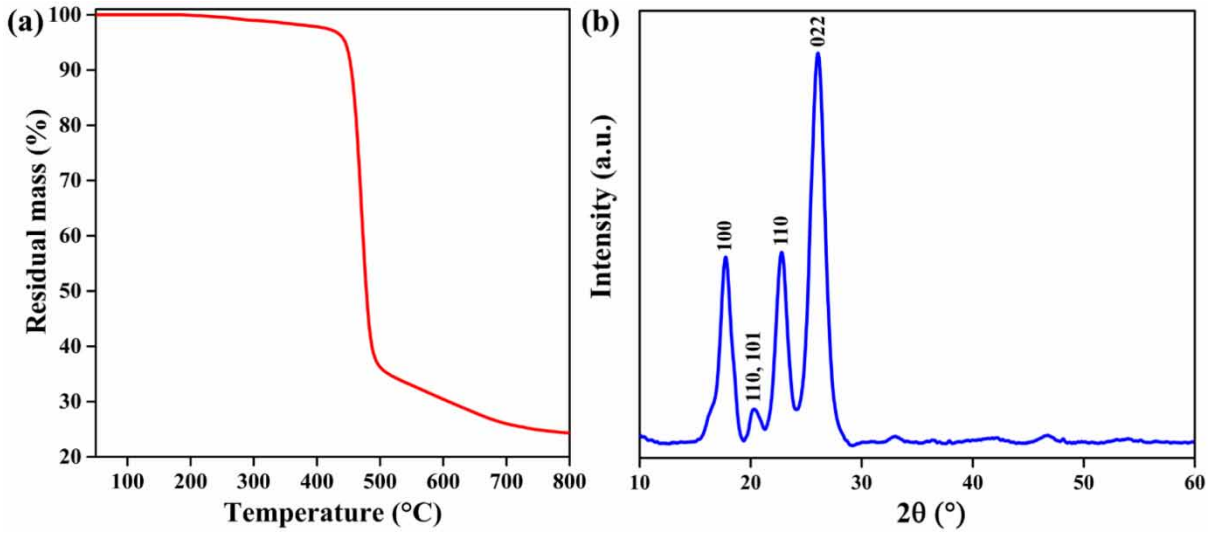

Figure 2 | (a) TGA thermogram and (b) XRD spectra of the recycled PVDF beads.

at $2\theta = 26.07°$ (022) were attributed to the γ- phase of the recycled PVDF phase. The peak at $2\theta = 20.03°$ was due to the combined β (110) and γ (101) phase (Martins *et al.* 2014; Esterly & Love 2004).

Figure 3 shows the FT-IR spectra of the recycled PVDF beads. The characteristic absorption bands at 1,400 and 1,180 cm^{-1} were due to C–H bending and C–F stretching, respectively. The absorbance band at 877 cm^{-1} was attributed to C–H wagging, while the absorbance band at 840 cm^{-1} was due to C–F bending (Daems *et al.* 2018; Yadav *et al.* 2021a, 2021b, 2021c). The absorbance bands at 839 and 870 cm^{-1} were attributed to the amorphous phase and at 1276 cm^{-1} to β-phase vibration (Zahirifar *et al.* 2019). The FT-IR analysis of the recycled PVDF beads confirmed no impurity in the recycled PVDF beads.

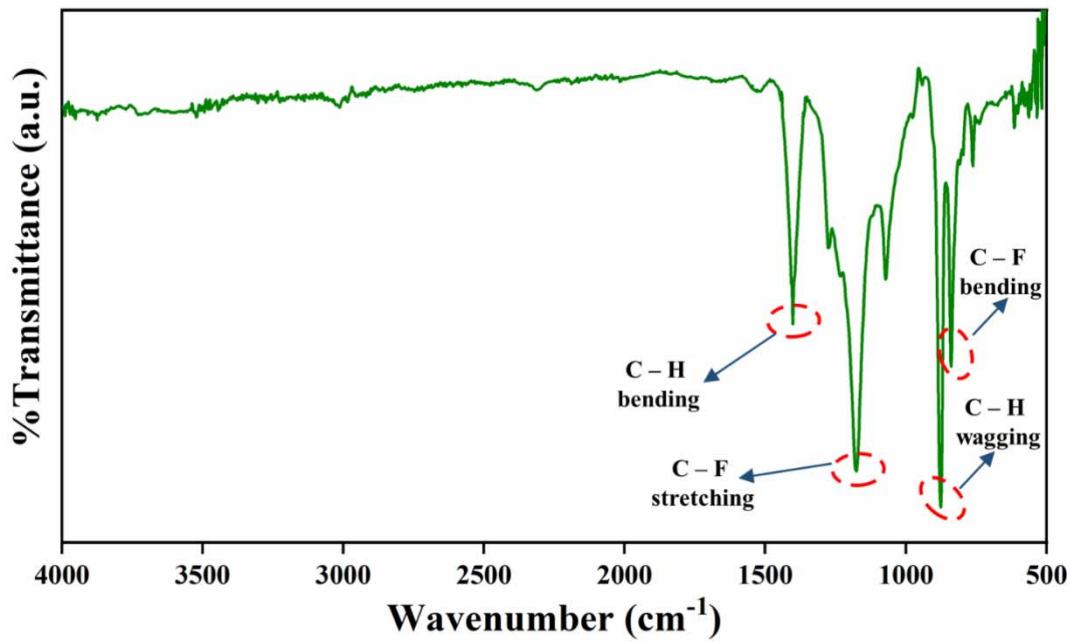

Figure 3 | FT-IR spectra of the recycled PVDF beads.

3.2. Adsorption experiments

The batch adsorption experiments were performed by varying one parameter at a time while the other parameters were kept constant. The effect of process parameters has been discussed in the subsequent sub-sections.

3.2.1. Effect of adsorbent dose

To remove MB dye with recycled PVDF beads, the influence of the adsorbent dose (0.2–3.0 g L^{-1}) was examined (Figure 4). The removal efficiency of MB dye increased from 25% to 99.10%, with an increase in adsorbent dose from 0.2 to 3 g L^{-1}. The increment in the removal efficiency was attributed to the increased availability of adsorption sites (Patel & Yadav 2022). After 2.5 g L^{-1} adsorbent dose, the removal efficiency reached the maximum value and remained constant on further increasing the dose. Although more active sites were available, no dye molecule was available in the solution to bind with the active adsorbent site due. The adsorption capacity of recycled PVDF beads decreased rapidly in the initial stages and steadily afterwards. As the number of recycled PVDF beads increased, the adsorption capacity decreased due to increased attraction forces, which led to the agglomeration of the beads (Mahmoudzadeh *et al.* 2013). In addition, the adsorption capacity decrement was due to increased excess active sites. The maximum adsorption capacity of active sites on recycled PVDF beads was not achieved because the concentration of the MB dye was fixed. Moreover, the adsorption capacity is inversely proportional to the adsorbent dose (Equation (1)). Similar observations are reported in other studies (Li *et al.* 2020; Shojaei & Esmaeili 2022).

3.2.2. Effect of pH

The effect of MB dye solution pH on the adsorption capacity and removal efficiency of the recycled PVDF beads was studied by varying the pH of the solution from 2 to 12. With the increased pH of MB dye solution, the removal efficiency increased from 55% to 99.20%, with the maximum removal efficiency at pH 10 (Figure 5). In a similar trend with an increase in MB dye solution pH, the adsorption capacity increased from 4.4 to 7.94 mg g^{-1}. This increase in removal efficiency and adsorption capacity can be explained by the negative charge present on the recycled PVDF beads (Chiao *et al.* 2020) and cationic MB dye. The removal efficiency increment was three stages. In the first stage (pH from 2 to 4), the removal efficiency increased slowly because the surface charge of the recycled PVDF was positive. In the second stage (pH from 4 to 8), the removal efficiency increased rapidly since the surface charge of the recycled PVDF became more negative. In the third

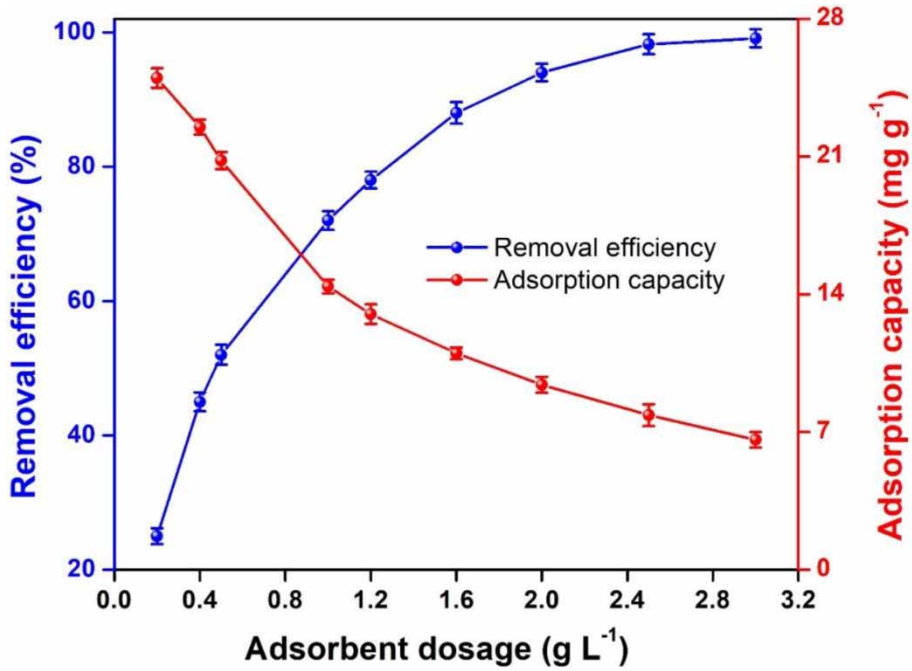

Figure 4 | Removal efficiency and adsorption capacity of recycled PVDF beads with varying adsorbent dosage (initial MB dye concentration: 20 ppm, contact time: 180 min, and pH: 7).

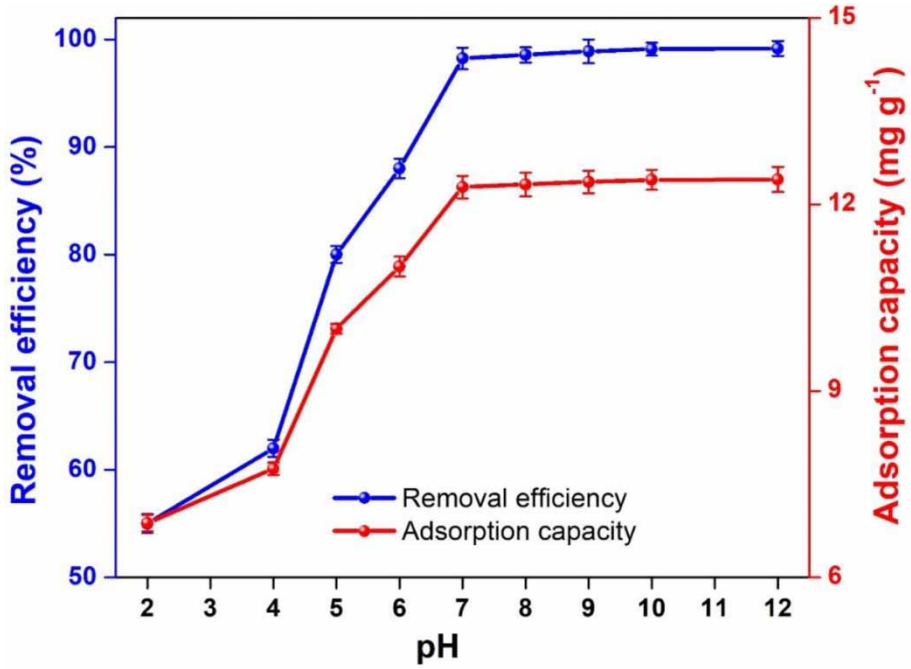

Figure 5 | Removal efficiency and adsorption capacity of recycled PVDF beads with varying pH (adsorbent dose: 2.5 g L^{-1}, initial MB dye concentration: 20 ppm, and contact time: 180 min).

stage (pH from 8 to 12), the removal efficiency increment was almost constant, attributed to the constant surface charge of the recycled PVDF.

3.2.3. Effect of contact time

The effect of recycled PVDF beads' contact time on the adsorption capacity and removal efficiency for MB dye adsorption was studied with varying contact times from 5 to 240 mins. The removal efficiency and adsorption capacity increased rapidly with the contact time of the adsorbent with dye solution and after some point of time, the curve becomes a plateau (Figure 6). The increments in removal efficiency and adsorption capacity were initially because of the availability of more active adsorption sites. As the adsorption process progressed, the active number of sites decreased as the adsorbent dose was fixed. Hence the curve becomes plateau with a maximum removal efficiency of 98.4%. Similar observations are reported in other studies (Geng *et al.* 2018; Yadav *et al.* 2022a, 2022b).

3.2.4. Effect of the initial MB concentration

The effect initial concentration of MB dye on removal efficiency and adsorption capacity was investigated by varying the initial concentration from 10 to 250 ppm. The removal efficiency decreased as the MB concentration increased (Figure 7). With increased MB dye concentration from 10 to 250 ppm, the removal efficiency reduced from 99.1% to 27.72%. This decrement in the removal efficiency was due to the increased interaction of MB dye with available active sites on recycled PVDF beads. The adsorption capacity increased from 3.96 to 27.72 mg g^{-1} with the MB dye initial concentration increasing from 10 to 250 ppm. The increased absorption capacity was attributed to the increased MB dye concentration. The adsorption capacity rose to 27.72 mg g^{-1} and remained constant because the adsorbent sites were fixed and the MB dye concentration increased (Liu *et al.* 2019; Jahan *et al.* 2021).

The maximum adsorption capacity of different adsorbents (mainly waste or recycled material) reported in the literature for the adsorption of the MB dye are compared with the maximum adsorption capacity of recycled PVDF beads in Table 1. The adsorption capacity of recycled PVDF beads was comparable with the reported adsorbents. This suggested the feasibility of the cost-effective recycled PVDF beads for the MB dye adsorption.

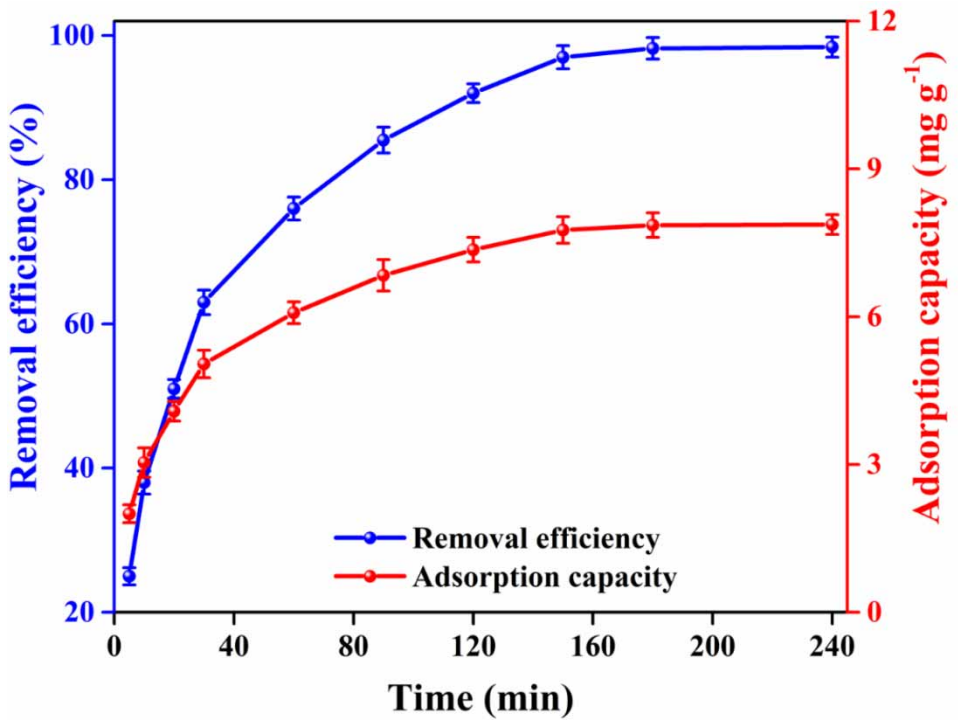

Figure 6 | Removal efficiency and adsorption capacity of recycled PVDF beads with varying contact time (adsorbent dose: 2.5 g L^{-1}, initial MB dye concentration: 20 ppm, and pH: 7).

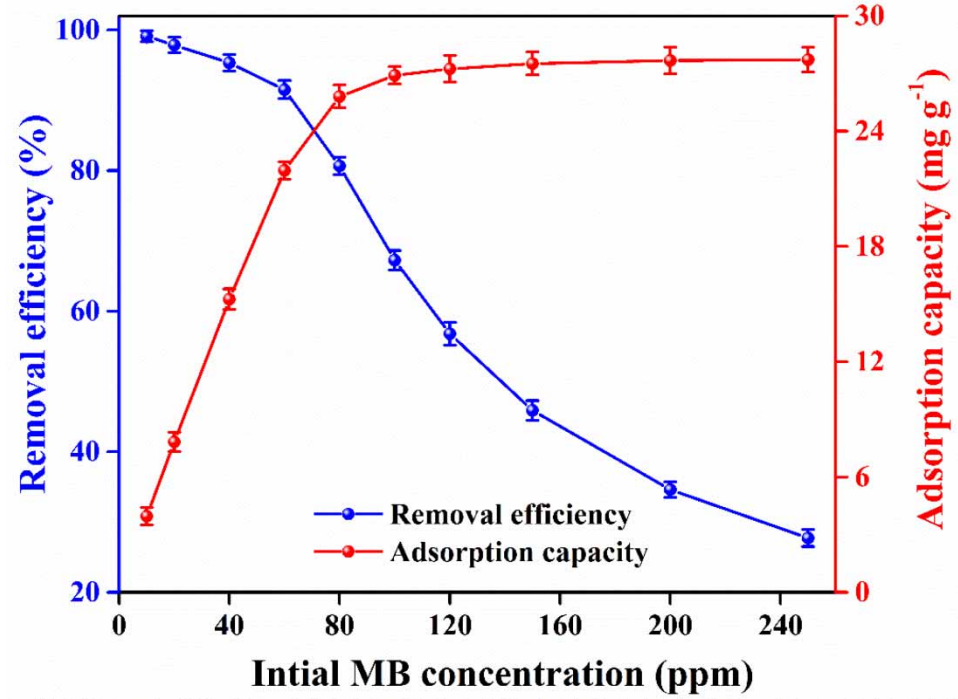

Figure 7 | Removal efficiency and adsorption capacity of recycled PVDF beads with varying initial concentrations of MB dye (adsorbent dose: 2.5 g L^{-1}, contact time: 180 min, and pH: 7).

Table 1 | Performance comparison of synthesized beads with previous works for adsorption of MB dye

Adsorbent	Dose (g L^{-1})	Contact time (min)	pH	Adsorption capacity (mg g^{-1})	Reference
Biochar	2.5	40	7.5	19	Yang *et al.* (2016)
Biochar microparticles (waste derived-pig manure)	0.5	–	7	16.30	Lonappan *et al.* (2016)
Mint waste	1	–	7.1	250	Ainane *et al.* (2014)
Bio-waste	0.2	120	7	135	Reddy *et al.* (2016)
Waste rice husk	0.2	45	7	18.7	Reddy *et al.* (2013)
Chemically treated cellulosic waste banana	0.8	1,440	5.6	250	Jawad *et al.* (2018)
Metroxylon (waste)	1	45	7	36.82	Amode *et al.* (2016)
Citrus limetta peel waste	2	180	9	227.3	Shakoor & Nasar (2016)
Potato (*Solanum tuberosum*) plant waste	2	25	7	52.6	Gupta *et al.* (2016)
Daucus carota (carrot leaves powder) waste	2	30	7	66.6	Kushwaha *et al.* (2014)
Date stones and palm-trees waste	10	240	6.3	40	Belala *et al.* (2011)
PVDF membrane	0.5	–	6.5	58.82	Bangari *et al.* (2022a, 2022b)
Recycled PVDF beads	2.5	180	7	27.86	This study

3.3. Adsorption kinetics and isotherm models

The optimization of the contact time of the adsorbent with the adsorbate molecules plays a significant role in adsorption studies to ensure complete equilibrium between the MB dye and recycled PVDF beads. The PFO and PSO models' adsorption kinetics were investigated to propose a plausible kinetic mechanism. Table 2 depicts different parameters of the PFO and PSO adoption kinetics for adsorption of MB dye on recycled PVDF beads. The correlation coefficient (R^2) for PFO and PSO models was 0.955 and 0.991, respectively. The R^2 value for PFO was far more unity than the PSO model, indicating the PSO non-linear second-order model fitting for the adsorption of MB dye on recycled PVDF beads. The PSO model fitting confirmed that the adsorption was chemical (Maslova *et al.* 2021). The value of the residual sum of the square and reduced chi-square was smaller from the PSO model than PFO. This was due to the lesser difference between the experimental and theoretical values for PSO and PFO models (Figure 8).

Two adsorption isotherms (Freundlich and Langmuir) were investigated for the adsorption of MB dye on recycled PVDF beads in the present study (Figure 9). The R^2, reduced chi-square, and residual sum of the square were calculated to predict the adsorption isotherm for MB adsorption on recycled PNDF beads (Table 3). The R^2 value was close to unity in the case for the Langmuir model (Freundlich: 0.843 and Langmuir: 0.991). The R^2 value was close to unity for the Langmuir isotherm model, indicating that the experimental data and predicted results obtained for the MB dye adsorption were closer. Moreover, the value of K_L was 0.767 (less than 1). If the value of K_L is between 0 and 1, the system can be considered suitable for adsorption purposes. In addition, the smaller value of the residual sum of square (6.965) makes this model applicable for the present work. The horizontal asymptote in the Langmuir isotherm indicated saturation after monolayer adsorption. The fitting Langmuir isotherm indicated the adsorption mechanism was chemical in nature of MB dye on recycled PVDF beads (Bangari *et al.* 2022a, 2022b).

Table 2 | PFO and PSO kinetics' parameter for MB dye adsorption on recycled PVDF beads

	PFO	PSO
q_e (mg g^{-1})	7.512	8.57
k (min^{-1})	0.039	0.006
R^2	0.955	0.991
Reduced chi-square	0.235	0.046
Residual sum of square	1.88	0.372

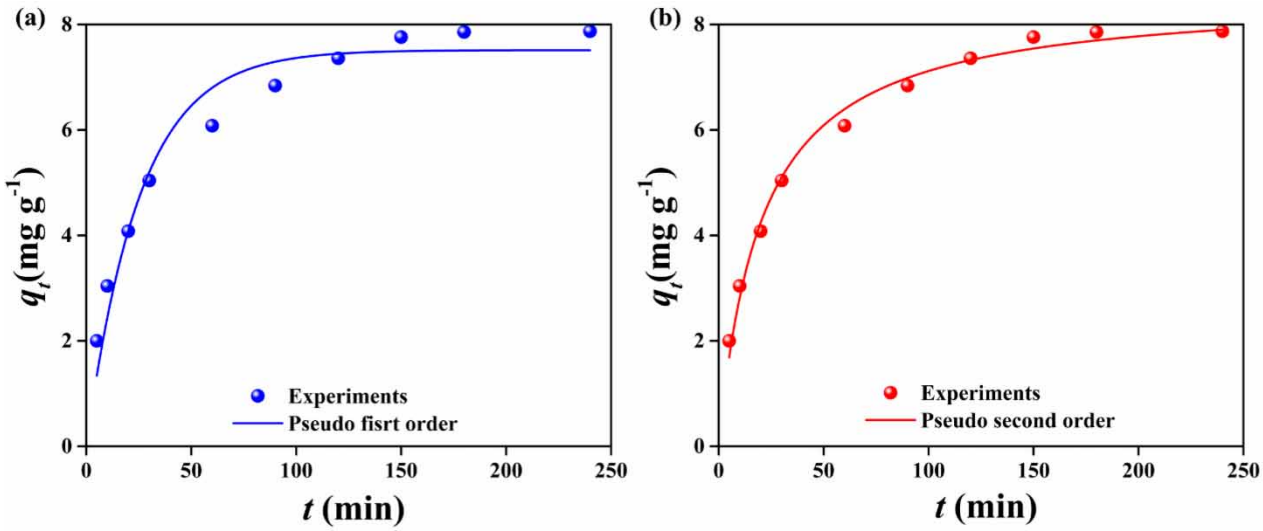

Figure 8 | Non-linear form of adsorption kinetics (a) PFO and (b) PSO.

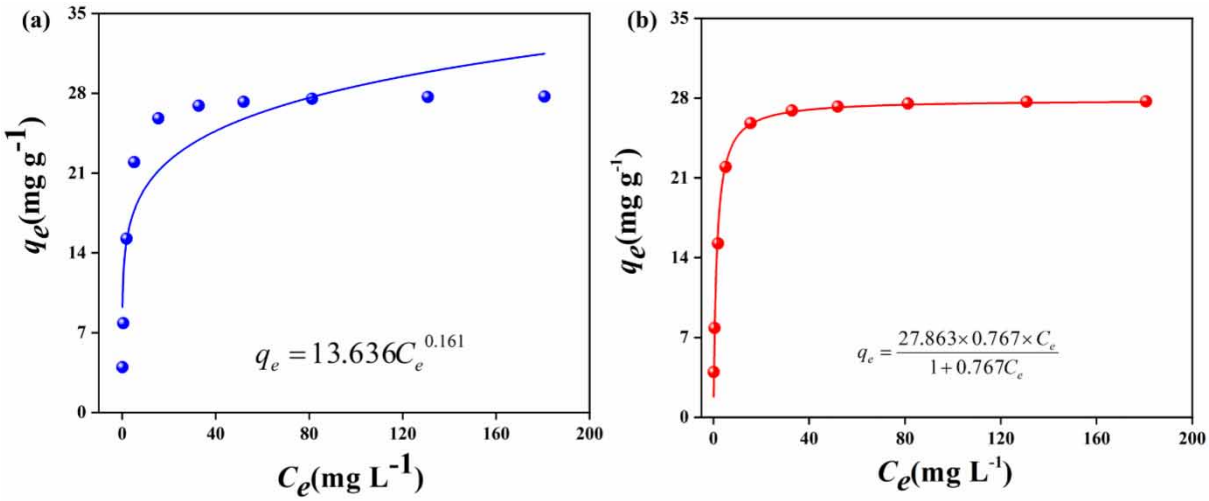

Figure 9 | Adsorption isotherms (a) Freundlich and (b) Langmuir.

Table 3 | Freundlich and Langmuir isotherm's parameter for MB dye adsorption on recycled PVDF beads

Freundlich isotherm	K_F ((mg g^{-1}) (L mg^{-1})$^{-1/n}$)	1/n	R^2	Reduced chi-square	Residual sum of squares
	13.636	0.161	0.843	14.247	113.978
Langmuir isotherm	q_m (mg g^{-1})	K_L (L mg^{-1})	R^2	Reduced chi-square	Residual sum of squares
	27.863	0.767	0.991	0.871	6.965

3.4. Computational analysis

The DFT optimized geometries of the PVDF, MB dye, and MB-PVDF clusters are shown in Figure 10. The relaxed non-planar geometries of PVDF and MB dye agreed with the literature (Bangari *et al.* 2022a, 2022b; Yadav *et al.* 2022a, 2022b). Several starting positions and orientations for the dye molecule were tested to find the most effective contact site. The N atom of MB

dye was closest to the PVDF at a distance of 3.21 Å. The adsorption energy for the MB-PVDF complex was –64.7 kJ mol^{-1} which described that the MB-PVDF system had positive interaction, supporting the experimental findings.

To determine the stability of the post adsorbed MB-PVDF complex, the vibrational frequencies of the PVDF, MB dye before and after adsorption complexes were computed (Figure 11(a)). All the PVDF and MB dye characteristic bands were present in their respective FT-IR spectra. After the interaction between PVDF and MB dye, the PVDF and MB dye bands were visible in the FT-IR of the MB-PVDF complex. As a result, the vibrational spectra indicated that the MB and PVDF interacted during adsorption. The number of electronic states per unit of energy in a material, as a function of energy, is provided by TDOS, which is critical for understanding its properties (Dindorkar *et al.* 2022b). The TDOS plots for PVDF, MB, and MB-PVDF clusters are shown in Figure 11(b). For the PVDF, the occupied and unoccupied molecular orbitals were widely spaced. After adsorption of MB dye on PVDF, additional energy levels appeared, which were traced to the charge transfer from the HOMO of the PVDF to the MB dye molecule. The adsorption of MB dye on PVDF resulted in a decrease in band

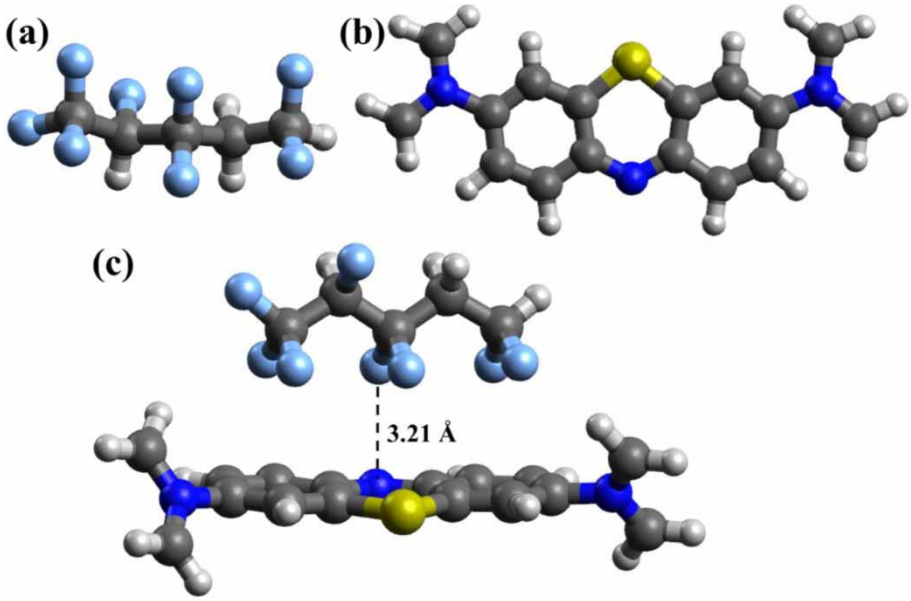

Figure 10 | DFT optimized geometries of (a) PVDF, (b) MB, and (c) MB-PVDF.

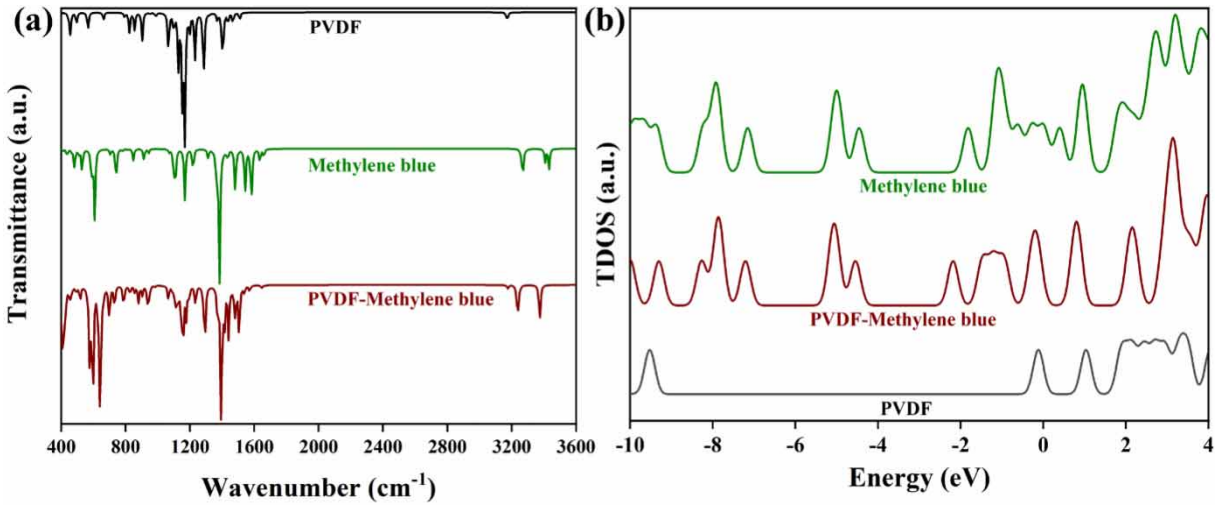

Figure 11 | (a) Theoretical IR spectra (b) TDOS of PVDF, MB, and PVDF-MB cluster.

gaps, which might be due to the emergence of new energy levels that mix the orbitals of MB dye molecules with the molecular orbitals of PVDF (Bangari *et al.* 2021). The TDOS plots confirmed the findings from the above sections and gave an account of the variation in the electronic density of states after the adsorption of MB dye.

The molecular orbitals (HOMO and LUMO) representation for PVDF, MB and PVDF-MB clusters are shown in Figure 12. The HOMOs and LUMOs were distributed uniformly on PVDF before adsorption. From the HOMO–LUMO, a reasonable charge distribution can be observed on the adsorbent sites on the double bond of the ethylene group. The HOMOs were concentrated on the electronegative N atoms of the MB dye molecule, while LUMOs were delocalized. After adsorption, the HOMOs and LUMOs were concentrated on MB dye molecules. This means that the MB-PVDF attained more nature of MB dye rather than PVDF. The HOMO and LUMO energies are related to chemical parameters that provide the details of the reactivity of the molecule (Dindorkar & Yadav 2022). Higher chemical stability can be attained with higher chemical hardness as they reduce the polarizability of the molecules. Therefore, as MB-PVDF's HOMO-LUMO energy gap (HLG) reduced after adsorption, chemical hardness also reduced, but there was little chemical potential change (Table 4). The HLG value of PVDF before and after adsorption was 9.42 eV and 0.50 eV, respectively. This was because of charge transfer

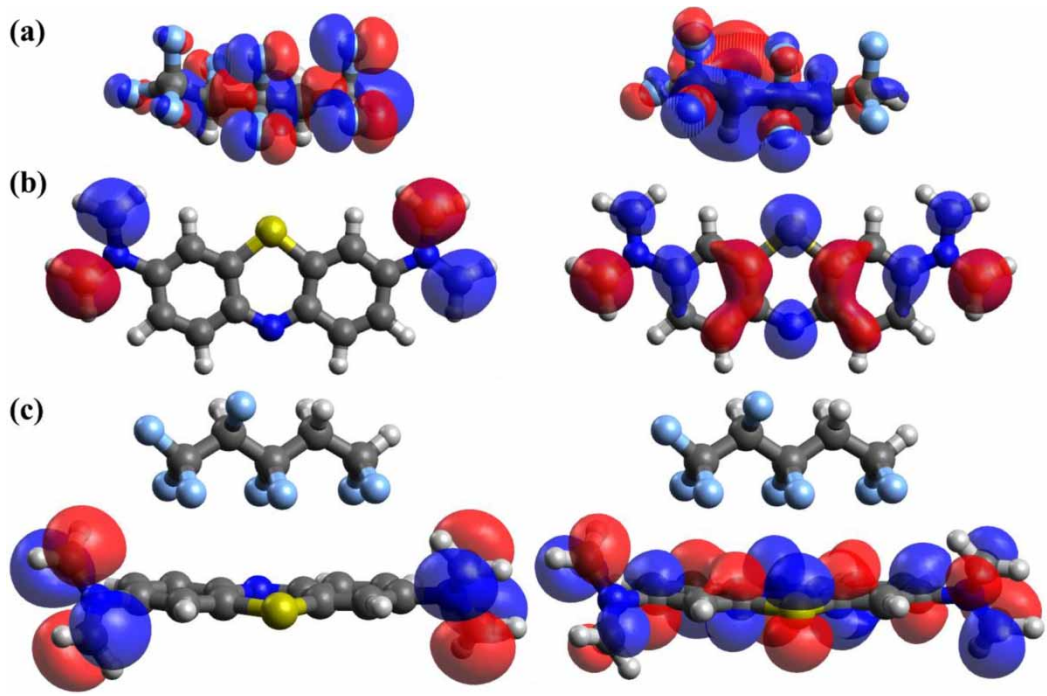

Figure 12 | HOMO-LUMO distributions on (a) PVDF, (b) MB, and (c) MB-PVDF.

Table 4 | The quantum mechanical descriptors before and after adsorption

Properties	PVDF	MB	MB-PVDF
HOMO	−9.53	−5.01	−4.95
LUMO	−0.11	−4.54	−4.45
HLG	9.42	0.47	0.50
VIP	9.53	5.01	4.95
VEA	0.11	4.54	4.45
Chemical hardness	4.71	0.24	0.25
Chemical potential	−4.82	−4.78	−4.70
Electrophilicity index	2.47	48.51	44.18

from MB dye to PVDF during adsorption, which led to a change in the density of occupied orbitals. As discussed above that the MB-PVDF complex attained the nature of MB dye, the complex became strong electrophile after absorption.

3.5. Plausible adsorption mechanism

Studying the adsorption mechanism of MB dye on recycled PVDF beads is important to gain insights into the actual process. Usually, if the PSO kinetic model describes an adsorption process better, it was inferred to be a chemisorption process. However, the DFT studies showed that the adsorption energy was -64 kJ mol^{-1}, implying the adsorption process was physical. Moreover, the shortest distance between the PVDF and MB dye molecules was >2 Å, implying that the adsorption was physical (Yadav & Dindorkar 2022a). As a result, the adsorption mechanism in this investigation could not be categorized solely as a chemical or physical response but rather as a mixed one. Other researchers have reported this observation (Zheng *et al.* 2018). MB dye is a cationic dye that gets adsorbed on the surface of the recycled PVDF beads by electrostatic attraction. The DFT simulations showed that the interaction of the MB dye molecule was from the electronegative N atom of the MB dye molecule. This means that electrostatic interaction occurred between the recycled PVDF beads and the positively charged quaternary ammonium groups in MB dye. The hydrogen bonding was due to the attraction between F atoms of PVDF and the amine group present in the MB dye molecule (Zheng *et al.* 2018). The adsorption was enhanced by the MB dye's linearity and three parallel aromatic rings, which encourage π-π interactions (Muslim *et al.* 2021).

4. CONCLUSIONS

In this study, we report the feasibility of the recycled PVDF for the adsorption of MB dye which mitigates two problems simultaneously: (i) disposal of used membranes and (ii) textile wastewater treatment. Batch adsorption experiments indicated that the MB dye adsorption onto the recycled PVDF beads depended on adsorbent dosage, initial concentration, contact time, and pH. The adsorption kinetics study of the MB dye adsorption followed the PSO model, indicating chemisorption. Furthermore, the adsorption isotherm study showed that the adsorption process followed the Langmuir isotherm showing the monolayer adsorption of MB dye on recycled PVDF beads. The PSO model's equilibrium adsorption capacity was 8.56 mg g^{-1}, and the experimental equilibrium adsorption capacity was 8.30 mg g^{-1}. The maximum adsorption capacity was 27.86 mg g^{-1}. The DFT study predicted the adsorption energy of –64.7 kJ mol^{-1} for MB-PVDF, indicating the strong interaction between MB dye and PVDF. Moreover, the gap between the HOMO and LUMO of PVDF upon interaction with MB dye decreased from 9.42 eV to 0.50 eV due to the mixing of molecular orbitals. The present study reveals the recycled PVDF beads' potential for textile wastewater dye removal at a low cost.

ACKNOWLEDGEMENTS

The CSIR-CSMCRI PRIS number for this manuscript is 109/2022. The authors are grateful for partial funding support from the Council of Scientific and Industrial Research, India (MLP-0043). The authors acknowledge AED&CIF division, CSIR-CSMCRI for providing instrumental facilities. The authors also thank Dr B. Ganguly, CSIR-CSMCRI, for his help in theoretical calculations. The comments from anonymous reviewers and the editor have greatly improved the content.

DATA AVAILABILITY STATEMENT

All relevant data are included in the paper or its Supplementary Information.

CONFLICTS OF INTEREST STATEMENT

The authors declare there is no conflict.

REFERENCES

Ainane, T., Khammour, F., Talbi, M. & Elkouali, M. 2014 A novel bio-adsorbent of mint waste for dyes remediation in aqueous environments: study and modeling of isotherms for removal of methylene blue. *Oriental Journal of Chemistry* **30** (3), 1183–1189.

Amode, J. O., Santos, J. H., Md. Alam, Z., Mirza, A. H. & Mei, C. C. 2016 Adsorption of methylene blue from aqueous solution using untreated and treated (Metroxylon spp.) waste adsorbent: equilibrium and kinetics studies. *International Journal of Industrial Chemistry* **7** (3), 333–345.

Bangari, R. S., Yadav, A. & Sinha, N. 2021 Experimental and theoretical investigations of methyl orange adsorption using boron nitride nanosheets. *Soft Matter* **17** (9), 2640–2651.

Bangari, R. S., Yadav, A., Awasthi, P. & Sinha, N. 2022a Experimental and theoretical analysis of simultaneous removal of methylene blue and tetracycline using boron nitride nanosheets as adsorbent. *Colloids and Surfaces A: Physicochemical and Engineering Aspects* **634**, 127943.

Bangari, R. S., Yadav, A., Bharadwaj, J. & Sinha, N. 2022b Boron nitride nanosheets incorporated polyvinylidene fluoride mixed matrix membranes for removal of methylene blue from aqueous stream. *Journal of Environmental Chemical Engineering* **10** (1), 107052.

Belala, Z., Jeguirim, M., Belhachemi, M., Addoun, F. & Trouvé, G. 2011 Biosorption of basic dye from aqueous solutions by date stones and palm-trees waste: kinetic, equilibrium and thermodynamic studies. *Desalination* **271** (1–3), 80–87.

Boys, S. F. & Bernardi, F. 1970 The calculation of small molecular interactions by the differences of separate total energies. Some procedures with reduced errors. *Molecular Physics* **19** (4), 553–566.

Caldeweyher, E., Bannwarth, C. & Grimme, S. 2017 Extension of the D3 dispersion coefficient model. *The Journal of Chemical Physics* **147** (3), 034112.

Chiao, Y.-H., Chen, S.-T., Sivakumar, M., Ang, M. B. M. Y., Patra, T., Almodovar, J., Wickramasinghe, S. R., Hung, W.-S. & Lai, J.-Y. 2020 Zwitterionic polymer brush grafted on polyvinylidene difluoride membrane promoting enhanced ultrafiltration performance with augmented antifouling property. *Polymers* **12** (6), 1303.

Coutinho de Paula, E., Gomes, J. C. L. & Amaral, M. C. S. 2017 Recycling of end-of-life reverse osmosis membranes by oxidative treatment: a technical evaluation. *Water Science and Technology* **76** (3), 605–622.

Daems, N., Milis, S., Verbeke, R., Szymczyk, A., Pescarmona, P. P. & Vankelecom, I. F. J. 2018 High-performance membranes with full pH-stability. *RSC Advances* **8** (16), 8813–8827.

Dindorkar, S. S. & Yadav, A. 2022 Insights from density functional theory on the feasibility of modified reactive dyes as dye sensitizers in dye-sensitized solar cell applications. *Solar* **2** (1), 12–31.

Dindorkar, S. S., Patel, R. V. & Yadav, A. 2022a Adsorptive removal of methylene blue dye from aqueous streams using photocatalytic CuBTC/ZnO chitosan composites. *Water Science and Technology* **85**, 2748–2760.

Dindorkar, S. S., Patel, R. V. & Yadav, A. 2022b Quantum chemical study of the defect laden monolayer boron nitride nanosheets for adsorption of pesticides from wastewater. *Colloids and Surfaces A: Physicochemical and Engineering Aspects* **643**, 128795.

Esterly, D. M. & Love, B. J. 2004 Phase transformation to?-poly(vinylidene fluoride) by milling. *Journal of Polymer Science Part B: Polymer Physics* **42** (1), 91–97.

Gan, D., Dou, J., Huang, Q., Huang, H., Chen, J., Liu, M., Qi, H., Yang, Z., Zhang, X. & Wei, Y. 2020 Carbon nanotubes-based polymer nanocomposites: bio-mimic preparation and methylene blue adsorption. *Journal of Environmental Chemical Engineering* **8** (2), 103525.

Geng, Y., Zhang, J., Zhou, J. & Lei, J. 2018 Study on adsorption of methylene blue by a novel composite material of TiO_2 and alum sludge. *RSC Advances* **8** (57), 32799–32807.

Gupta, N., Kushwaha, A. K. & Chattopadhyaya, M. C. 2016 Application of potato (Solanum tuberosum) plant wastes for the removal of methylene blue and malachite green dye from aqueous solution. *Arabian Journal of Chemistry* **9**, S707–S716.

Ivanets, A. I., Prozorovich, V. G., Roshchina, M. Y., Srivastava, V. & Sillanpää, M. 2019 Unusual behavior of MgFe2O4 during regeneration: desorption versus specific adsorption. *Water Science and Technology* **80** (4), 654–658.

Jahan, K., Tyeb, S., Kumar, N. & Verma, V. 2021 Bacterial cellulose-polyaniline porous mat for removal of methyl orange and bacterial pathogens from potable water. *Journal of Polymers and the Environment* **29** (4), 1257–1270.

Janakiraman, S., Surendran, A., Ghosh, S., Anandhan, S. & Venimadhav, A. 2016 Electroactive poly(vinylidene fluoride) fluoride separator for sodium ion battery with high coulombic efficiency. *Solid State Ionics* **292**, 130–135.

Jawad, A. H., Rashid, R. A., Ishak, M. A. M. & Ismail, K. 2018 Adsorptive removal of methylene blue by chemically treated cellulosic waste banana (Musa sapientum) peels. *Journal of Taibah University for Science* **12** (6), 809–819.

Kiran, S., Ahmad, T., Gulzar, T., Ashraf, A., Naqvi, S. A. R. & Naz, S. 2020 Agro-waste applications for bioremediation of textile effluents. In: *Recycling From Waste in Fashion and Textiles* (Pandit, P., Ahmed, S., Singha, K. & Shrivastava, S. eds.). Wiley, Beverly, MA 01915, United States. pp. 391–421.

Kushwaha, A. K., Gupta, N. & Chattopadhyaya, M. C. 2014 Removal of cationic methylene blue and malachite green dyes from aqueous solution by waste materials of Daucus carota. *Journal of Saudi Chemical Society* **18** (3), 200–207.

Lawler, W., Bradford-Hartke, Z., Cran, M. J., Duke, M., Leslie, G., Ladewig, B. P. & Le-Clech, P. 2012 Towards new opportunities for reuse, recycling and disposal of used reverse osmosis membranes. *Desalination* **299**, 103–112.

Li, H., Liu, L., Cui, J., Cui, J., Wang, F. & Zhang, F. 2020 High-efficiency adsorption and regeneration of methylene blue and aniline onto activated carbon from waste edible fungus residue and its possible mechanism. *RSC Advances* **10** (24), 14262–14273.

Liu, Y., Huang, Y., Xiao, A., Qiu, H. & Liu, L. 2019 Preparation of magnetic Fe3O4/MIL-88A nanocomposite and its adsorption properties for bromophenol blue dye in aqueous solution. *Nanomaterials* **9** (1), 51.

Lonappan, L., Rouissi, T., Das, R. K., Brar, S. K., Ramirez, A. A., Verma, M., Surampalli, R. Y. & Valero, J. R. 2016 Adsorption of methylene blue on biochar microparticles derived from different waste materials. *Waste Management* **49**, 537–544.

Mahmoudzadeh, M., Fassihi, A., Emami, J., Davies, N. M. & Dorkoosh, F. 2013 Physicochemical, pharmaceutical and biological approaches toward designing optimized and efficient hydrophobically modified chitosan-based polymeric micelles as a nanocarrier system for targeted delivery of anticancer drugs. *Journal of Drug Targeting* **21** (8), 693–709.

Manoj Kumar Reddy, P., Mahammadunnisa, S., Ramaraju, B., Sreedhar, B. & Subrahmanyam, C. 2013 Low-cost adsorbents from bio-waste for the removal of dyes from aqueous solution. *Environmental Science and Pollution Research* **20** (6), 4111–4124.

Martins, P., Lopes, A. C. & Lanceros-Mendez, S. 2014 Electroactive phases of poly(vinylidene fluoride): determination, processing and applications. *Progress in Polymer Science* **39** (4), 683–706.

Maslova, M., Mudruk, N., Ivanets, A., Shashkova, I. & Kitikova, N. 2021 The effect of pH on removal of toxic metal ions from aqueous solutions using composite sorbent based on Ti-Ca-Mg phosphates. *Journal of Water Process Engineering* **40**, 101830.

Mok, C. F., Ching, Y. C., Muhamad, F., Abu Osman, N. A., Hai, N. D. & Che Hassan, C. R. 2020 Adsorption of dyes using poly(vinyl alcohol) (PVA) and PVA-based polymer composite adsorbents: a review. *Journal of Polymers and the Environment* **28** (3), 775–793.

Muslim, M., Ali, A., Neogi, I., Dege, N., Shahid, M. & Ahmad, M. 2021 Facile synthesis, topological study, and adsorption properties of a novel Co (II)-based coordination polymer for adsorptive removal of methylene blue and methyl orange dyes. *Polyhedron* **210**, 115519.

Ngulube, T., Gumbo, J. R., Masindi, V. & Maity, A. 2017 An update on synthetic dyes adsorption onto clay based minerals: a state-of-art review. *Journal of Environmental Management* **191**, 35–57.

Obotey Ezugbe, E., Rathilal, S., Ezugbe, E. O., Rathilal, S., Obotey Ezugbe, E. & Rathilal, S. 2020 Membrane technologies in wastewater treatment: a review. *Membranes* **10** (5), 89.

O'Boyle, N. M., Tenderholt, A. L. & Langner, K. M. 2008 Cclib: a library for package-independent computational chemistry algorithms. *Journal of Computational Chemistry* **29** (5), 839–845.

Park, S., Kang, J.-S., Lee, J., Vo, T.-K.-Q. & Kim, H.-S. 2018 Application of physical and chemical enhanced backwashing to reduce membrane fouling in the water treatment process using ceramic membranes. *Membranes* **8** (4), 110.

Piaskowski, K., Świderska-Dąbrowska, R. & Zarzycki, P. K. 2018 Dye removal from water and wastewater using various physical, chemical, and biological processes. *Journal of AOAC International* **101** (5), 1371–1384.

Reddy, P. M. K., Verma, P. & Subrahmanyam, C. 2016 Bio-waste derived adsorbent material for methylene blue adsorption. *Journal of the Taiwan Institute of Chemical Engineers* **58**, 500–508.

Shakoor, S. & Nasar, A. 2016 Removal of methylene blue dye from artificially contaminated water using citrus limetta peel waste as a very low cost adsorbent. *Journal of the Taiwan Institute of Chemical Engineers* **66**, 154–163.

Shojaei, M. & Esmaeili, H. 2022 Ultrasonic-assisted synthesis of zeolite/activated carbon@MnO2 composite as a novel adsorbent for treatment of wastewater containing methylene blue and brilliant blue. *Environmental Monitoring and Assessment* **194** (4), 279.

Su, H., Li, W., Han, Y. & Liu, N. 2018 Magnetic carboxyl functional nanoporous polymer: synthesis, characterization and its application for methylene blue adsorption. *Scientific Reports* **8** (1), 6506.

Temesgen, F., Gabbiye, N. & Sahu, O. 2018 Biosorption of reactive red dye (RRD) on activated surface of banana and orange peels: economical alternative for textile effluent. *Surfaces and Interfaces* **12**, 151–159.

Tran, H. N., Nguyen, H. C., Woo, S. H., Nguyen, T. V., Vigneswaran, S., Hosseini-Bandegharaei, A., Rinklebe, J., Kumar Sarmah, A., Ivanets, A., Dotto, G. L., Bui, T. T., Juang, R.-S. & Chao, H.-P. 2019 Removal of various contaminants from water by renewable lignocellulose-derived biosorbents: a comprehensive and critical review. *Critical Reviews in Environmental Science and Technology* **49** (23), 2155–2219.

Vardhan Patel, R. & Yadav, A. 2022 Photocatalytic MIL101(Fe)/ZnO chitosan composites for adsorptive removal of tetracycline antibiotics from the aqueous stream. *Journal of Molecular Structure* **1252**, 132128.

Vecino, X., Devesa-Rey, R., Cruz, J. M. & Moldes, A. B. 2015 Study of the physical properties of calcium alginate hydrogel beads containing vineyard pruning waste for dye removal. *Carbohydrate Polymers* **115**, 129–138.

Wallingford, C. T. 2013 Gaussian, Inc..

Wong, S., Ghafar, N. A., Ngadi, N., Razmi, F. A., Inuwa, I. M., Mat, R. & Amin, N. A. S. 2020 Effective removal of anionic textile dyes using adsorbent synthesized from coffee waste. *Scientific Reports* **10** (1), 2928.

Yadav, A. & Dindorkar, S. S. 2022a Adsorption behaviour of hexagonal boron nitride nanosheets towards cationic, anionic and neutral dyes: insights from first principle studies. *Colloids and Surfaces A: Physicochemical and Engineering Aspects* **640**, 128509.

Yadav, A. & Dindorkar, S. S. 2022b Vacancy defects in monolayer boron carbon nitride for enhanced adsorption of paraben compounds from aqueous stream: a quantum chemical study. *Surface Science* **723**, 122131.

Yadav, A. & Sinha, N. 2021 Organic polymers for drinking water purification. In: *Reference Module in Materials Science and Materials Engineering*. Elsevier.

Yadav, A., Labhasetwar, P. K. & Shahi, V. K. 2021a Fabrication and optimization of tunable pore size poly(ethylene glycol) modified poly(vinylidene-co-hexafluoropropylene) membranes in vacuum membrane distillation for desalination. *Separation and Purification Technology* **271**, 118840.

Yadav, A., Patel, R. V. R. V., Labhasetwar, P. K. P. K. & Shahi, V. K. V. K. 2021b Novel MIL101(Fe) impregnated poly(vinylidene fluoride-co-hexafluoropropylene) mixed matrix membranes for dye removal from textile industry wastewater. *Journal of Water Process Engineering* **43**, 102317.

Yadav, A., Sharma, P., Panda, A. B. & Shahi, V. K. 2021c Photocatalytic TiO2 incorporated PVDF-co-HFP UV-cleaning mixed matrix membranes for effective removal of dyes from synthetic wastewater system via membrane distillation. *Journal of Environmental Chemical Engineering* **9** (5), 105904.

Yadav, A., Dindorkar, S. S., Ramisetti, S. B. & Sinha, N. 2022a Simultaneous adsorption of methylene blue and arsenic on graphene, boron nitride and boron carbon nitride nanosheets: insights from molecular simulations. *Journal of Water Process Engineering* **46**, 102653.

Yadav, P., Yadav, A. & Labhasetwar, P. K. 2022b Sustainable adsorptive removal of antibiotics from aqueous streams using Fe_3O_4-functionalized MIL101(Fe) chitosan composite beads. *Environmental Science and Pollution Research* **29**, 37204 –37217.

Yanai, T., Tew, D. P. & Handy, N. C. 2004 A new hybrid exchange–correlation functional using the Coulomb-attenuating method (CAM-B3LYP). *Chemical Physics Letters* **393** (1–3), 51–57.

Yang, G., Wu, L., Xian, Q., Shen, F., Wu, J. & Zhang, Y. 2016 Removal of Congo red and methylene blue from aqueous solutions by vermicompost-derived biochars. *PLoS ONE* **11** (5), 1–18.

Yaseen, D. A. & Scholz, M. 2019 Textile dye wastewater characteristics and constituents of synthetic effluents: a critical review. *International Journal of Environmental Science and Technology* **16** (2), 1193–1226.

Yi, X., Wang, Y., Jin, L. & Shi, W. 2017 Critical flux investigation in treating o/w emulsion by TiO2/Al2O3-PVDF UF membrane. *Water Science and Technology* **76** (10), 2785–2792.

Zahirifar, J., Hadi, A., Karimi-Sabet, J. & Dastbaz, A. 2019 Influence of hexagonal boron nitride nanosheets as the additives on the characteristics and performance of PVDF for air gap membrane distillation. *Desalination* **460**, 81–91.

Zhang, D., Dai, F., Zhang, P., An, Z., Zhao, Y. & Chen, L. 2019 The photodegradation of methylene blue in water with PVDF/GO/ZnO composite membrane. *Materials Science and Engineering: C* **96**, 684–692.

Zheng, X., Zheng, H., Zhao, R., Sun, Y., Sun, Q., Zhang, S. & Liu, Y. 2018 Polymer-functionalized magnetic nanoparticles: synthesis, characterization, and methylene blue adsorption. *Materials* **11** (8), 1312.

Zwain, H. M., Vakili, M. & Dahlan, I. 2014 Waste material adsorbents for zinc removal from wastewater: a comprehensive review. *International Journal of Chemical Engineering* **2014**, 1–13.

First received 14 April 2022; accepted in revised form 8 June 2022. Available online 17 June 2022